J|A|C|S ARTICLES

Published on Web 10/15/2009

Turn-On Fluorescence Detection of Cyanide in Water: Activation of Latent Fluorophores through Remote Hydrogen Bonds That Mimic Peptide β-Turn Motif

Junyong Jo and Dongwhan Lee*

Department of Chemistry, Indiana University, 800 East Kirkwood Avenue, Bloomington, Indiana 47405

Received August 20, 2009; E-mail: dongwhan@indiana.edu

Abstract: A molecular probe was prepared that selectively responds to cyanide in aqueous solutions by fluorescence enhancement. Using the peptide β-turn as a structural template, we designed a series of diphenylacetylene derivatives in which the π-conjugated backbone was functionalized with an aldehyde group to render the molecule nonfluorescent. The N−H···O hydrogen bond across the 2,2′-functionalized diphenylacetylene turn motif activates the carbonyl group toward nucleophilic attack, and chemical transformation of this internal quencher site by reaction with CN^- elicits a rapid ($k = 72$ M^{-1} s^{-1}) enhancement in the emission at $\lambda_{max} = 375$ nm. Tethering of an ammonium group to the hydrogen bond donor fragment significantly increased both the response kinetics and the intensity of the fluorescence signal. In addition to providing electrostatic attraction toward the CN^- ion, this positively charged R-NH_3^+ fragment can engage in a secondary hydrogen bond to facilitate the formation of the cyanohydrin adduct responsible for the signaling event. The structurally optimized molecular probe **3** responds exclusively to μM-level cyanide in neutral aqueous solutions, with no interference from other common anions including F^- and AcO^-.

Introduction

Cyanide is a toxic anion that binds heme cofactors to inhibit the terminal respiratory chain enzyme cytochrome *c* oxidase.[1] Cellular hypoxia resulting from such an event often leads to fatal consequences. Uptake of CN^- also raises the concentration of intracellular Ca^{2+} to trigger a cascade of enzymatic events to increase the level of reactive oxygen species (ROS) and inhibit antioxidant defense systems.[2,3] The widespread use of cyanide in industrial settings (1.5 million tons per year)[1] and potential threats for terrorism continue to engender significant research efforts directed toward its detection under biologically relevant conditions.

Cyanide ion can function as a Lewis base or a nucleophile. Accordingly, detection schemes that capitalize on either property have been pursued using a diverse array of structural platforms. For example, a direct coordination of CN^- to electron-deficient trivalent boron perturbs the [p,π*]-conjugation[4] or internal charge transfer (ICT) pathways,[5] and thereby modifies the optical properties of the cyanoboryl adduct. The strong donor ability of cyanide is also exploited for coordination to transition metal centers[6−8] or demetalation of preassembled complexes[9−13] to elicit detectable changes in absorption or emission spectra. Alternatively, nucleophilic attack of CN^- on activated carbonyl groups[14−20] or heterocyclic ring systems[21−24] can irreversibly modify the probe molecule with concomitant changes in optical properties.[25]

(1) Bhattacharya, R.; Flora, S. J. S. In *Handbook of Toxicology of Chemical Warfare Agents*; Gupta, R. C., Ed.; Academic Press: Boston, 2009; pp 255−270.
(2) Johnson, J. D.; Meisenheimer, T. L.; Isom, G. E. *Toxicol. Appl. Pharmacol.* **1986**, *84*, 464–469.
(3) Ardelt, B. K.; Borowitz, J. L.; Isom, G. E. *Toxicology* **1989**, *56*, 147–154.
(4) (a) Hudnall, T. W.; Gabbaï, F. P. *J. Am. Chem. Soc.* **2007**, *129*, 11978–11986. (b) Kim, Y.; Zhao, H.; Gabbaï, F. P. *Angew. Chem., Int. Ed.* **2009**, *48*, 4957–4960.
(5) Badugu, R.; Lakowicz, J. R.; Geddes, C. D. *J. Am. Chem. Soc.* **2005**, *127*, 3635–3641.
(6) Kim, Y.-H.; Hong, J.-I. *Chem. Commun.* **2002**, 512–513.
(7) Chow, C.-F.; Lam, M. H. W.; Wong, W.-Y. *Inorg. Chem.* **2004**, *43*, 8387–8393.
(8) (a) Zelder, F. H. *Inorg. Chem.* **2008**, *47*, 1264–1266. (b) Männel-Croisé, C.; Zelder, F. *Inorg. Chem.* **2009**, *48*, 1272–1274.
(9) Lou, X.; Zhang, L.; Qin, J.; Li, Z. *Chem. Commun.* **2008**, 5848–5850.
(10) Touceda-Varela, A.; Stevenson, E. I.; Galve-Gasión, J. A.; Dryden, D. T. F.; Mareque-Rivas, J. C. *Chem. Commun.* **2008**, 1998–2000.
(11) Zeng, Q.; Cai, P.; Li, Z.; Qin, J.; Tang, B. Z. *Chem. Commun.* **2008**, 1094–1096.
(12) Li, Z. a.; Lou, X.; Yu, H.; Li, Z.; Qin, J. *Macromolecules* **2008**, *41*, 7433–7439.
(13) Shang, L.; Zhang, L.; Dong, S. *Analyst* **2009**, *134*, 107–113.
(14) Ros-Lis, J. V.; Martínez-Máñez, R.; Soto, J. *Chem. Commun.* **2002**, 2248–2249.
(15) (a) Chung, Y. M.; Raman, B.; Kim, D.-S.; Ahn, K. H. *Chem. Commun.* **2006**, 186–188. (b) Chung, Y.; Lee, H.; Ahn, K. H. *J. Org. Chem.* **2006**, *71*, 9470–9474. (c) Miyaji, H.; Kim, D.-S.; Chang, B.-Y.; Park, E.; Park, S.-M.; Ahn, K. H. *Chem. Commun.* **2008**, 753–755. (d) Lee, H.; Chung, Y. M.; Ahn, K. H. *Tetrahedron Lett.* **2008**, *49*, 5544–5547.
(16) Chen, C.-L.; Chen, Y.-H.; Chen, C.-Y.; Sun, S.-S. *Org. Lett.* **2006**, *8*, 5053–5056.
(17) Lee, K.-S.; Kim, H.-J.; Kim, G.-H.; Shin, I.; Hong, J.-I. *Org. Lett.* **2008**, *10*, 49–51.
(18) (a) Sessler, J. L.; Cho, D.-G. *Org. Lett.* **2008**, *10*, 73–75. (b) Cho, D.-G.; Kim, J. H.; Sessler, J. L. *J. Am. Chem. Soc.* **2008**, *130*, 12163–12167.
(19) Ekmekci, Z.; Yilmaz, M. D.; Akkaya, E. U. *Org. Lett.* **2008**, *10*, 461–464.

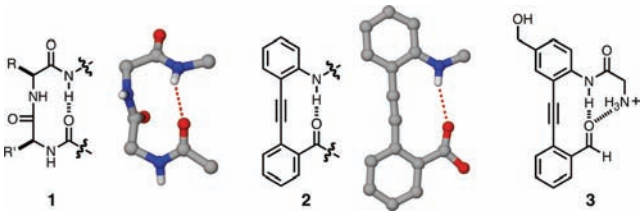

Figure 1. Chemical structures of peptide β-turn (**1**), its synthetic mimic (**2**), and cyanide probe **3** built on 2,2′-functionalized diphenylacetylene template. Solid-state structures generated using CSD codes ADUCEH (for **1**) and WUTVOW (for **2**) are shown for comparison, in which side chains and N/O substituents have been removed for clarity. Hydrogen bonds are denoted with dotted lines.

Despite the increasing number of proof-of-principle molecular prototypes, however, few cyanide detection systems operate in genuine aqueous environment with turn-on response.[5,10,17] Taking inspirations from naturally occurring β-turn motif **1**[26−28] and its structural mimic **2**,[29−32] we have designed a diphenylacetylene-based cyanide probe **3** (Figure 1), which (i) operates in water at pH = 6−8, (ii) responds by fluorescence enhancement with fast response kinetics (k = 72 M^{-1} s^{-1}) and μM-level detection limit, and (iii) displays high selectivity without interference from other common anions including fluoride and acetate. Comparative studies on a series of structural analogues provided significant insights into the structural and functional role of intramolecular hydrogen bonds in mechanism-based cyanide probes, which constitute the main topic of this paper.

Background: Hydrogen Bonds for Anion Detection. Converging arrays of N−H or O−H hydrogen bond donor (HBD) groups have been studied extensively for anion sensing.[33−44] In these elaborate receptor molecules, multiple X−H···Y^- (X−H = HBD group; Y^- = anion) contacts are achieved by positioning of X−H groups as part of the macrocyclic backbone or on the concave side of crescent-shaped hosts. In addition to functioning as the recognition sites for Lewis basic anions, HBD groups have also been exploited in a growing number of reactivity-based CN^- indicators,[25] in which covalent modification of the reporter molecule is facilitated by HBD functioning as an internal activating group.

Scheme 1. Reactivity-Based Detection of CN^- by Nucleophilic Attack on Hydrogen-Bonded Carbonyl Groups

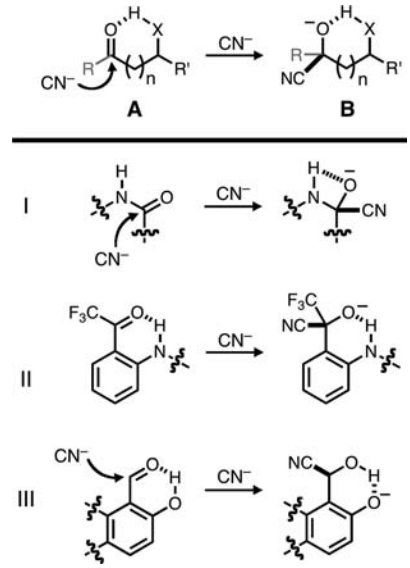

As shown in Scheme 1, nucleophilic attack by CN^- on the carbonyl group of a latent chromophore **A** converts it to the cyanohydrin adduct **B** having different absorption/emission properties. The efficiency of this reactivity-based detection scheme can significantly be improved by positioning a HBD group to stabilize the developing negative charge on the carbonyl oxygen atom. In addition to facilitating the functionally requisite chemical transformation, the resulting X−H···O^- motif in **B** rigidifies the molecule by restricting internal torsional motions,[45] which can further enhance the emission quantum yield.[46,47]

The feasibility of this reactivity-based detection scheme has been demonstrated by a number of fluorogenic molecular probes that respond to CN^- (Scheme 1). Either the N−H···O hydrogen bond in **I**[16,19,20] and **II**[15a,c,d,48] or the O−H···O hydrogen bond in **III**[17,24] facilitates the formation of cyanohydrin from nucleophilic attack by CN^-, a process that is often assisted by the electron-withdrawing trifluoromethyl substituent on the carbonyl

(20) Niu, H.-T.; Su, D.; Jiang, X.; Yang, W.; Yin, Z.; He, J.; Cheng, J.-P. *Org. Biomol. Chem.* **2008**, *6*, 3038–3040.
(21) (a) Tomasulo, M.; Raymo, F. M. *Org. Lett.* **2005**, *7*, 4633–4636. (b) Tomasulo, M.; Sortino, S.; White, A. J. P.; Raymo, F. M. *J. Org. Chem.* **2006**, *71*, 744–753.
(22) García, F.; García, J. M.; García-Acosta, B.; Martínez-Máñez, R.; Sancenón, F.; Soto, J. *Chem. Commun.* **2005**, 2790–2792.
(23) Yang, Y.-K.; Tae, J. *Org. Lett.* **2006**, *8*, 5721–5723.
(24) Lee, K.-S.; Lee, J. T.; Hong, J.-I.; Kim, H.-J. *Chem. Lett.* **2007**, *36*, 816–817.
(25) Cho, D.-G.; Sessler, J. L. *Chem. Soc. Rev.* **2009**, *38*, 1647–1662.
(26) Sibanda, B. L.; Blundell, T. L.; Thornton, J. M. *J. Mol. Biol.* **1989**, *206*, 759–777.
(27) Burgess, K. *Acc. Chem. Res.* **2001**, *34*, 826–835.
(28) Robinson, J. A. *Acc. Chem. Res.* **2008**, *41*, 1278–1288.
(29) (a) Kemp, D. S.; Li, Z. Q. *Tetrahedron Lett.* **1995**, *36*, 4175–4178. (b) Kemp, D. S.; Li, Z. Q. *Tetrahedron Lett.* **1995**, *36*, 4179–4180.
(30) Cary, J. M.; Moore, J. S. *Org. Lett.* **2002**, *4*, 4663–4666.
(31) (a) Yang, X.; Brown, A. L.; Furukawa, M.; Li, S.; Gardinier, W. E.; Bukowski, E. J.; Bright, F. V.; Zheng, C.; Zeng, X. C.; Gong, B. *Chem. Commun.* **2003**, 56–57. (b) Yang, X.; Yuan, L.; Yamato, K.; Brown, A. L.; Feng, W.; Furukawa, M.; Zeng, X. C.; Gong, B. *J. Am. Chem. Soc.* **2004**, *126*, 3148–3162.
(32) Hu, W.; Zhu, N.; Tang, W.; Zhao, D. *Org. Lett.* **2008**, *10*, 2669–2672.
(33) Miyaji, H.; Sessler, J. L. *Angew. Chem., Int. Ed.* **2001**, *40*, 154–157.
(34) Gale, P. A. *Coord. Chem. Rev.* **2001**, *213*, 79–128.
(35) Beer, P. D.; Gale, P. A. *Angew. Chem., Int. Ed.* **2001**, *40*, 486–516.
(36) Lavigne, J. J.; Anslyn, E. V. *Angew. Chem., Int. Ed.* **2001**, *40*, 3118–3130.
(37) Martínez-Máñez, R.; Sancenón, F. *Chem. Rev.* **2003**, *103*, 4419–4476.
(38) (a) Best, M. D.; Tobey, S. L.; Anslyn, E. V. *Coord. Chem. Rev.* **2003**, *240*, 3–15. (b) Sessler, J. L.; Camiolo, S.; Gale, P. A. *Coord. Chem. Rev.* **2003**, *240*, 17–55. (c) Llinares, J. M.; Powell, D.; Bowman-James, K. *Coord. Chem. Rev.* **2003**, *240*, 57–75. (d) Bondy, C. R.; Loeb, S. J. *Coord. Chem. Rev.* **2003**, *240*, 77–99. (e) Choi, K.; Hamilton, A. D. *Coord. Chem. Rev.* **2003**, *240*, 101–110. (f) Gale, P. A. *Coord. Chem. Rev.* **2003**, *240*, 191–221.
(39) Suksai, C.; Tuntulani, T. *Chem. Soc. Rev.* **2003**, *32*, 192–202.
(40) Cho, W.-S.; Sessler, J. L. In *Functional Synthetic Receptors*; Schrader, T., Hamilton, A. D., Eds.; Wiley-VCH: Weinheim, Germany, 2005; pp 165−256.
(41) Bowman-James, K. *Acc. Chem. Res.* **2005**, *38*, 671–678.
(42) Amendola, V.; Esteban-Gómez, D.; Fabbrizzi, L.; Licchelli, M. *Acc. Chem. Res.* **2006**, *39*, 343–353.
(43) Caltagirone, C.; Gale, P. A. *Chem. Soc. Rev.* **2009**, *38*, 520–563.
(44) Anzenbacher, P., Jr.; Tyson, D. S.; Jursíková, K.; Castellano, F. N. *J. Am. Chem. Soc.* **2002**, *124*, 6232–6233.
(45) (a) Jiang, X.; Bollinger, J. C.; Lee, D. *J. Am. Chem. Soc.* **2006**, *128*, 11732–11733. (b) Riddle, J. A.; Jiang, X.; Huffman, J.; Lee, D. *Angew. Chem., Int. Ed.* **2007**, *46*, 7019–7022.
(46) Turro, N. J. *Modern Molecular Photochemistry*; University Science Books: Sausalito, CA, 1991.
(47) Valeur, B. *Molecular Fluorescence: Principles and Applications*; Wiley-VCH: Weinheim, Germany, 2002.
(48) Peng, L.; Wang, M.; Zhang, G.; Zhang, D.; Zhu, D. *Org. Lett.* **2009**, *11*, 1943–1946.

Scheme 2. Cartoon-Type Representation of the Fluorophore−Quencher−Activator Triad Organized through Intramolecular Hydrogen Bonds, and Chemical Structures of **3**−**5**

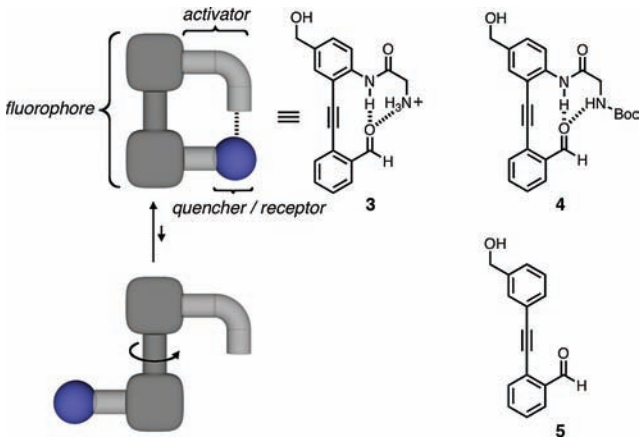

carbon.[19,20,15a,c,d,48] Formation of such cyanide adduct entails either diminution (= turn-off) or, more desirably, enhancement (= turn-on) in the emission intensity of the reporter group. Among these hydrogen-bonding assisted cyanide-detecting probes, only one system operates in genuine aqueous environment with turn-on fluorescence response.[17]

Results and Discussion

Design and Synthesis. As shown in Figure 1, an appropriately functionalized diphenylacetylene **2** can restrict C−C bond rotation along the molecular axis. A robust β-turn mimic[49−56] based on this structural motif was pioneered by Kemp[29] and subsequently exploited as a conformational lock to assist structural folding and rigidification of phenyleneethylene-based oligomers.[30−32] We envisioned that a simple aldehyde group could be placed within a similar structural context to furnish **3**, in which the 2,2′-functionalized diphenylacetylene backbone functions as a π-extended fluorogenic group (Scheme 2). As in typical aromatic carbonyls, a rapid intersystem crossing from [n,π*] singlet-state to [π,π*] triplet-state would render the molecule nonfluorescent,[57,58] but chemical transformation of the carbonyl group to cyanohydrin (Scheme 1) should suppress the internal quenching process and restore the intrinsic fluorescence associated with diphenylacetylene. We anticipated that such fluorescence "turn-on" scheme could be exploited for detection of CN^-. In addition, comparative studies on a series of structural analogues **3**−**5** (Scheme 2), which share a common π-conjugated backbone but differ in the number of N−H···O hydrogen bonds and the overall charge, would provide significant insights into the structure−function relationships.

Scheme 3. Synthetic Routes to **3**−**5**[a]

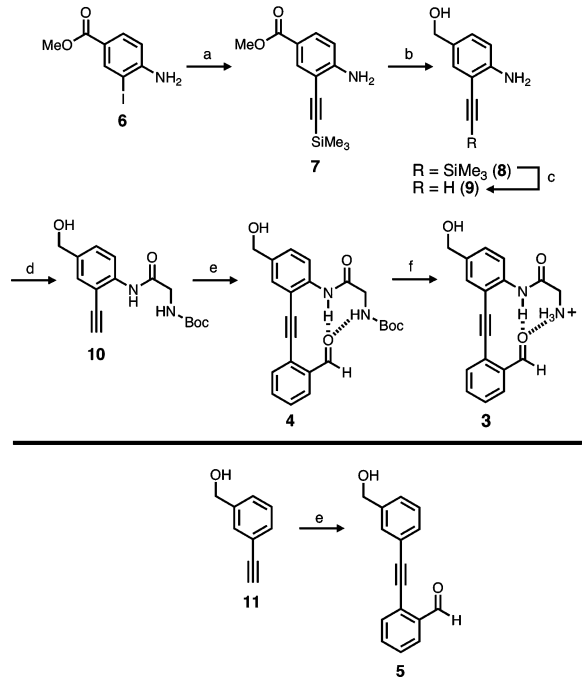

[a] Reagents and conditions: (a) $HCCSiMe_3$, $Pd(PPh_3)_2Cl_2$, CuI, $^iPr_2NH$, THF, r.t., 82%. (b) $LiAlH_4$, THF, 0 °C, 78%. (c) TBAF, THF/H_2O, 50 °C, >99%. (d) EDC, Boc-Gly, CH_2Cl_2, 40 °C, 83%. (e) 2-Iodobenzaldehyde, $Pd(PPh_3)_2Cl_2$, CuI, $^iPr_2NH$, THF, r.t. 92% for **4**; 78% for **5**. (f) HCl, CH_2Cl_2, 0 °C, >99%.

Our synthesis commenced with installation of a protected acetylene fragment onto a known ester **6** (Scheme 3). The ester functionality in the coupling product **7** was reduced to an alcohol group to enhance water solubility (of the products **3** and **4**). A standard EDC-mediated amide coupling with Boc-protected glycine converted **9** to **10**, which was subjected to a Sonogashira-Hagihara coupling with 2-iodobenzaldehyde to furnish **4**. Subsequent deprotection of the Boc group provided **3** as a pale yellow solid material in an overall 48% yield in six steps from known materials. Compound **5**, lacking the hydrogen-bonding donor motif, was also prepared in a straightforward manner (Scheme 3).

Solution Structures Probed by NMR Spectroscopy. An important consideration in the design of **3** is distal hydrogen bonding between the aldehyde carbonyl and the N−H groups across the "turn" motif (Figure 1 and Scheme 2). Experimental evidence for this functionally required (Scheme 1) noncovalent interaction was obtained by solution ^1H NMR spectroscopic studies. In DMSO-d_6 at 298 K, **3** (4.5 mM) displays downfield proton resonances at 10.44, 10.16, and 8.40 ppm, which are assigned to the aldehyde C−H, amide N−H, and ammonium N−H protons, respectively (Figure 2a). Notably, the aniline amide N−H resonance of **3** at 10.16 ppm is significantly ($\Delta\delta \approx 1$ ppm) downfield-shifted relative to that of **10** (Scheme 3) at 9.13 ppm (Figure 2c), which implicates deshielding from hydrogen-bonding interaction with the carbonyl group across the turn motif.[59−61]

(49) Kemp, D. S.; Bowen, B. R.; Muendel, C. C. *J. Org. Chem.* **1990**, *55*, 4650–4657.
(50) Diaz, H.; Espina, J. R.; Kelly, J. W. *J. Am. Chem. Soc.* **1992**, *114*, 8316–8318.
(51) Smith, A. B.; Guzman, M. C.; Sprengeler, P. A.; Keenan, T. P.; Holcomb, R. C.; Wood, J. L.; Carroll, P. J.; Hirschmann, R. *J. Am. Chem. Soc.* **1994**, *116*, 9947–9962.
(52) Brandmeier, V.; Sauer, W. H. B.; Feigel, M. *Helv. Chim. Acta* **1994**, *77*, 70–85.
(53) Ogawa, M. Y.; Gretchikhine, A. B.; Soni, S.-D.; Davis, S. M. *Inorg. Chem.* **1995**, *34*, 6423–6424.
(54) Loughlin, W. A.; Tyndall, J. D. A.; Glenn, M. P.; Fairlie, D. P. *Chem. Rev.* **2004**, *104*, 6085–6118.
(55) Nowick, J. S. *Org. Biomol. Chem.* **2006**, *4*, 3869–3885.
(56) Wyrembak, P. N.; Hamilton, A. D. *J. Am. Chem. Soc.* **2009**, *131*, 4566–4567.
(57) El-Sayed, M. A. *Acc. Chem. Res.* **1968**, *1*, 8–16.
(58) de Silva, A. P.; Gunaratne, H. Q. N.; Gunnlaugsson, T.; Huxley, A. J. M.; McCoy, C. P.; Rademacher, J. T.; Rice, T. E. *Chem. Rev.* **1997**, *97*, 1515–1566.
(59) Jeffrey, G. A. *An Introduction to Hydrogen Bonding*; Oxford University Press: New York, NY, 1997.

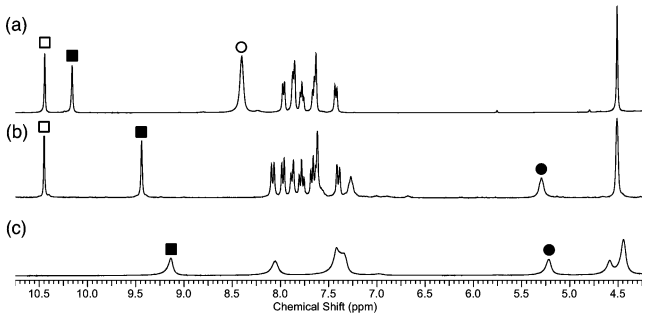

Figure 2. Partial ^{1}H NMR spectra of (a) **3**, (b) **4**, and (c) **10** in DMSO-d_6. Sample concentrations = 4.5 mM; T = 298 K. The symbols □, ■, ○, and ● indicate the resonances of the aldehyde C−H, aniline amide N−H, ammonium N−H, and Boc amide N−H proton, respectively.

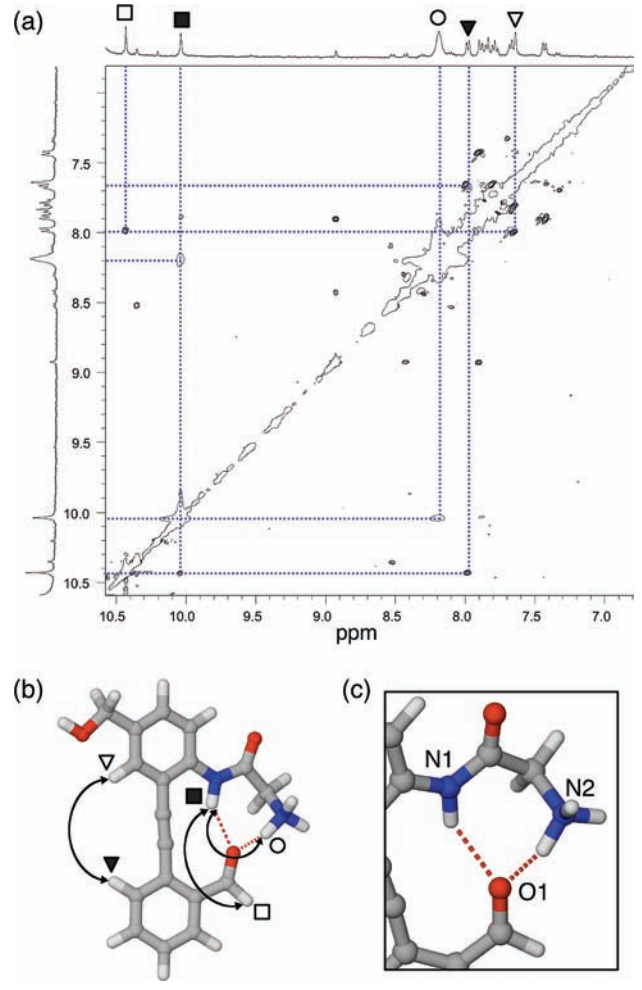

Figure 3. (a) Partial 2D-ROESY spectrum of **3** (4.5 mM) in DMSO-d_6 solution at T = 298 K. (b) Capped-stick representation of the DFT (B3LYP/6-31G**) geometry optimized model of **3**, and (c) a close-up view showing hydrogen bonds (dotted red lines) and ROE contacts (double-headed arrows). The protons contributing to the cross-peaks denoted in (a) are labeled with the corresponding symbols. Selected interatomic distances: N1···O1 = 3.110 Å; N2···O1 = 2.613 Å.

In support of this notion, the 2D-ROESY ^{1}H NMR spectrum (Figure 3a) taken in DMSO-d_6 revealed correlation between the amide N−H, ammonium N−H, and aldehyde C−H protons that are brought in close proximity through the N−H···O=C contact.[29] A geometry-optimized model of **3**, generated by density functional theory (DFT) calculations with the B3LYP functional and the 6-31G** basis set (Figure 3b,c),[62] is also consistent with this observation. The presence of similar bifurcated hydrogen bonds[59−61] in **4** (Scheme 2) was evidenced by significantly downfield-shifted N−H proton resonances at 9.38 ppm (for aniline amide) and 5.50 ppm (for Boc-amide) in $CDCl_3$, relative to the corresponding signals at 8.65 ppm and 5.19 ppm determined for **10**. In DMSO-d_6, however, these values change to 9.43 ppm and 5.28 ppm for **4** (Figure 2b) and 9.13 ppm and 5.22 ppm for **10** (Figure 2c). This trend presumably reflects weaker intramolecular hydrogen bond donor ability of the bulky Boc-amide N−H group compared with the aniline amide N−H group and, therefore, less pronounced spectral shift ($\Delta\delta$) in hydrogen-bonding solvent DMSO.

The strength of the intramolecular hydrogen-bonding network in **3** (Scheme 2) was assessed by concentration-dependent ^{1}H NMR studies. The N−H proton resonances of **3** in DMSO-d_6 remain essentially invariant within the concentration range of 0.2−6.0 mM but, beyond this point, display systematic downfield shifts with increasing concentration (Figure S1). This concentration-dependent changes in chemical shifts of both amide N−H proton (from 10.05 to 10.16 ppm) and ammonium N−H proton (from 8.22 to 8.40 ppm) can best be explained by the formation of intermolecular hydrogen bonds, which becomes competitive with intramolecular hydrogen bonds only at high concentrations. Apparently, a combination of (i) positive charge, (ii) less steric constraints, and (iii) multiple N−H donor units are responsible for the strong propensity of **3** to engage in hydrogen bonds, the functional relevance of which was probed further in the reaction with CN^-.

Reaction with Cyanide in Water. With solution ^{1}H NMR evidence obtained for the intramolecular hydrogen bonding and its stability in polar solvent environment ($E_T(30)$ = 45.1 for DMSO),[63,64] we initiated investigating the reactivity of **3** toward CN^-. Specifically, we wished to establish that (i) N−H···O=C hydrogen bonds across the β-turn mimic can facilitate nucleophilic attack on the carbonyl group by CN^-, (ii) this chemical transformation on the side chain can restore the inherent fluorescence of the π-conjugated molecular backbone, and (iii) such reactivity-based turn-on detection can be implemented in an aqueous environment at physiologically relevant pH.

Preliminary studies established a linear correlation between the absorbance and concentration of **3** up to 70 μM in H_2O (Figure S2), indicating good water solubility and no interchromophore interactions in solution within the concentration range of 0−70 μM. Accordingly, all UV−vis (with [**3**] = 50 μM) and fluorescence (with [**3**] = 5.0 μM) measurements were conducted for aqueous solution samples at pH = 7.0 (HEPES, 10 mM). As shown in Figure 4, **3** displays a strong electronic transition at $\lambda_{max,abs}$ = 350 nm ($\varepsilon = 1.21 \times 10^4$ M^{-1} cm^{-1}) but is only weakly fluorescent with emission quantum yield of Φ_F = 1.3% when excited at λ_{exc} = 270 nm. Addition of NaCN

(60) Prins, L. J.; Reinhoudt, D. N.; Timmerman, P. *Angew. Chem., Int. Ed.* **2001**, *40*, 2382–2492.
(61) Steiner, T. *Angew. Chem., Int. Ed.* **2002**, *41*, 48–76.
(62) (a) *Jaguar*, v7.0; Schrödinger LLC: New York, NY, 2007. (b) Becke, A. D. *Phys. Rev. A* **1988**, *38*, 3098–3100. (c) Becke, A. D. *J. Chem. Phys.* **1993**, *98*, 5648–5652. (d) Vosko, S. H.; Wilk, L.; Nusair, M. *Can. J. Phys.* **1980**, *58*, 1200–1211. (e) Lee, C. T.; Yang, W. T.; Parr, R. G. *Phys. Rev. B* **1988**, *37*, 785–789. (f) Stephens, P. J.; Devlin, F. J.; Chabalowski, C. F.; Frisch, M. J. *J. Phys. Chem.* **1994**, *98*, 11623–11627.
(63) Reichardt, C. *Chem. Rev.* **1994**, *94*, 2319–2358.
(64) Reichardt, C. *Solvents and Solvent Effects in Organic Chemistry*, 3rd ed.; Wiley-VCH: Weinheim, 2003.

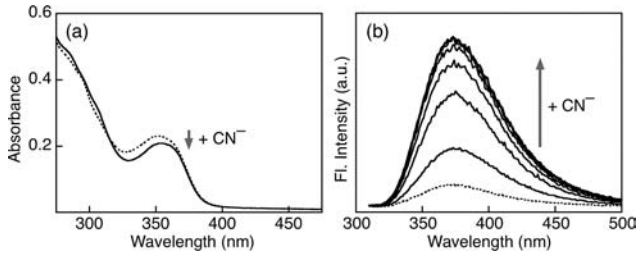

Figure 4. (a) Electronic absorption spectra of **3** (= 50 μM) prior to (dotted line) and after (solid line) addition of NaCN (30 equiv). (b) Fluorescence response of **3** (= 5.0 μM; λ_{exc} = 270 nm) toward increasing amount of NaCN, with spectral traces corresponding to [NaCN] = 0, 0.2, 0.5, 0.7, 0.9, 1.2, and 1.5 mM from bottom to top. All measurements were conducted in water at pH = 7.0 (HEPES, 10 mM).

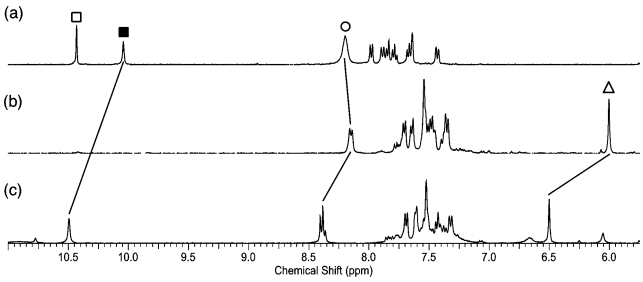

Figure 5. Partial ^{1}H NMR spectra of (a) **3** in DMSO-d_6, (b) **3** + 5 equiv NaCN in DMSO-d_6/D_2O (5:2, v/v), and (c) **3** + 5 equiv (n-Bu_4N)CN in DMSO-d_6; [**3**] = 4.5 mM, T = 298 K. The symbols □, ■, ○, and △ indicate the resonances of the aldehyde C−H, aniline amide N−H, ammonium N−H, and benzylic C−H proton, respectively. The lines indicate some corresponding signals. In (b), the amide N−H proton resonance disappears as a result of H/D exchange with D_2O.

(300 equiv) to the aqueous solution of **3**, however, elicited a significant (>7-fold) enhancement in the emission (Φ_F = 10%) at $\lambda_{max,em}$ = 375 nm (Figure 4b), with only a slight decrease in absorption intensity (Figure 4a).

The reaction between **3** and cyanide was further analyzed by a continuous variation method (= Job's plot; Figure S3) to determine a 1:1 reaction stoichiometry. A LC-MS analysis of the reaction mixture of **3** and NaCN in H_2O at pH = 7.0 (HEPES, 10 mM; Figure S4) revealed two major components, which were identified as **3** (calculated for $[\mathbf{3}]^+$, 309.1239; found, 309.1249) and its cyanide adduct (calculated for $[\mathbf{3} + CN + H]^+$, 336.1348; found, 336.1352) based on high-resolution MS analysis (Figures S5 and S6). Addition of NaCN (5 equiv) in D_2O to a DMSO-d_6 solution (4.5 mM) of **3** resulted in the disappearance of the aldehyde proton signal at 10.44 ppm with concomitant development of a new resonance at 6.00 ppm, which was assigned to a benzylic proton (Figure 5b). Addition of cyanide (5 equiv) as a tetrabutylammonium salt resulted in a similar spectral change, with the benzylic proton of the reaction product appearing at 6.50 ppm with complete disappearance of the aldehyde signal of the starting material (Figure 5c). Notably, the amide N−H proton resonance of the reaction product at 10.49 ppm (Figure 5c) is significantly downfield shifted from that (10.16 ppm) of **3**, which implicates a stronger deshielding from the newly developing hydrogen bond in the cyanide adduct of **3**.

The spectroscopic and mass-spectrometric data described above are fully consistent with direct nucleophilic attack by CN^- on the aldehyde group of **3** to form a cyanohydrin adduct **3a**

Scheme 4. Detection of Cyanide by **3** through the Formation of Fluorescent Cyanohydrin Adduct **3a**

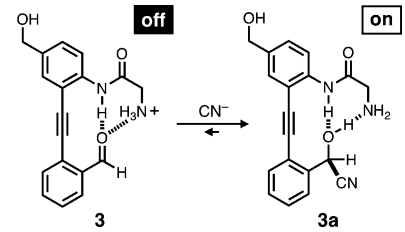

Scheme 5. Mechanism of Fluorescence Turn-On Detection of CN^- by Quencher-Modified Quantum Dot (Top) or by Quencher-Modified Fluorescent Dye Molecule, Such as **3** (Bottom)

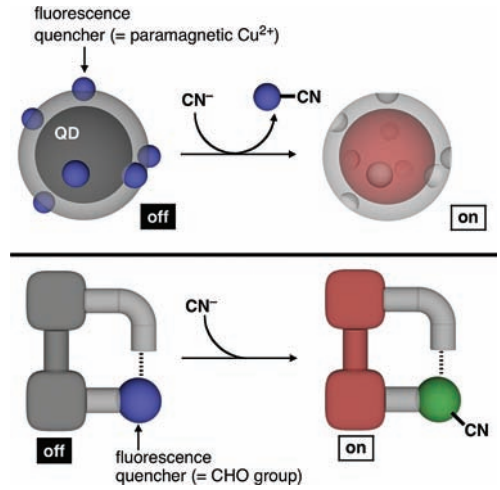

(Scheme 4).[65] Stabilization of the developing negative charge in **3a** by multiple N−H groups should facilitate the forward step in this inherently reversible reaction.

An efficient chemical transformation of the quencher group by CN^- restores the fluorescence of the π-conjugated molecular backbone of **3** functioning as a reporter group. A conceptual linkage can be drawn to cyanide detection schemes implemented with fluorescent quantum dots (QDs),[10,13] in which the reporter remains nonluminescent in the presence of paramagetic quencher Cu^{2+} ion. Coordination of CN^- dissociates the metal ion from the QD surface and thereby elicits a turn-on response (Scheme 5).

Kinetics of CN^- Signaling and Structure−Property Relationships. Detection of cyanide ion through the reaction shown in Scheme 4 critically relies on the efficiency of nucleophilic attack of cyanide on the carbonyl group of **3**. Under pseudo-first-order conditions ($[NaCN]_0 > 100[\mathbf{3}]$), an exponential increase in the emission intensity (= ΔI_{375nm}; λ_{exc} = 270 nm) was observed from the reaction between **3** and cyanide in H_2O (pH = 7.0; HEPES, 10 mM) at 298 K (Figure 6a). A linear dependence of the pseudo-first-order rate constant k' (= $k[CN^-]_0$; eq 1) on $[CN^-]_0$ (Figures 6b and S7) indicates a rate-limiting C−C bond formation by nucleophilic attack of CN^- on **3** with the second-order rate constant of k = 72 M^{-1} s^{-1}.

$$\frac{\Delta I}{I} = 1 - e^{-k't} \qquad (1)$$

The functional role of intramolecular hydrogen bonds in this bimolecular reaction was probed further by using the compounds

(65) In aqueous solution, an equilibrium between **3a** and its N-protonated form might also be established.

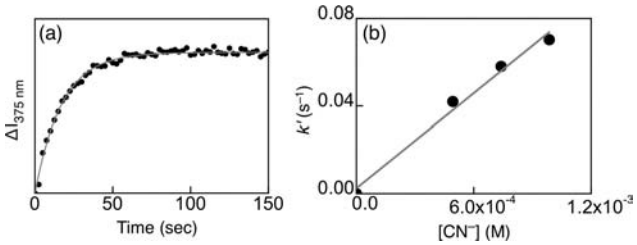

Figure 6. (a) Time-dependent changes in the fluorescence intensity at $\lambda = 375$ nm ($\lambda_{exc} = 270$ nm) observed from the reaction between **3** (5.0 μM) and NaCN (0.74 mM) in H_2O (pH = 7.0; HEPES, 10 mM) at $T = 298$ K. The gray curve overlaid on the experimental data points is theoretical fit generated using $k' = 5.8 \times 10^{-2}$ s^{-1}. (b) A plot of k' ($= k[CN^-]_0$) vs $[CN^-]_0$ to derive the second-order rate constant $k = 72$ M^{-1} s^{-1}.

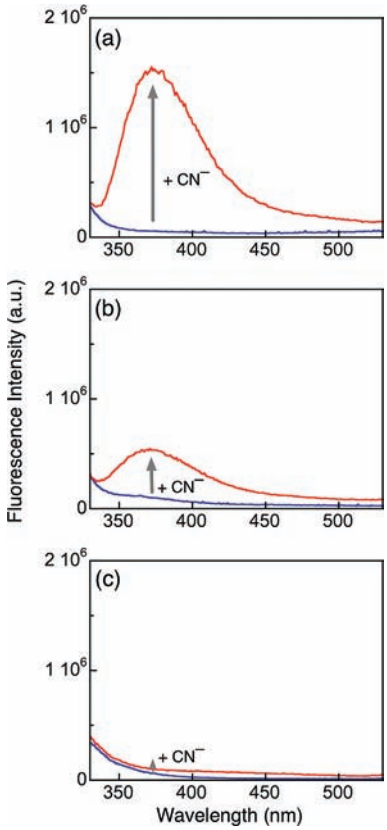

Figure 7. Changes in the emission spectra of 5.0 μM solution samples of (a) **3**, (b) **4**, and (c) **5**, prior to (blue) and after (red) addition of NaCN (300 equiv) in MeCN. $\lambda_{exc} = 270$ nm; $T = 298$ K.

3−**5** (Scheme 2). Due to the limited solubility of **4** and **5** in H_2O, all comparative reactivity and kinetic studies were conducted in MeCN. As shown in Figure 7, the efficiency of cyanide detection, as judged by ΔI_{375nm} upon introduction of the same amount of NaCN to the solution samples (5.0 μM) of the probes, follows the trend of **3** > **4** ≫ **5**. The largest fluorescence enhancement was observed for **3** having charge-assisted hydrogen bond, whereas **5** having a simple non-hydrogen-bonded aldehyde group shows essentially no reactivity toward CN^-.[66]

Subsequent kinetic studies revealed that, in addition to the larger signal response (Figure 7a,b), **3** reacts about 7 times faster than **4** toward CN^-, with second-order rate constants of 91 M^{-1} s^{-1} (for **3**) and 13 M^{-1} s^{-1} (for **4**) determined at 288 K (Figures S8 and S9). The markedly (7-fold) enhanced reactivity of **3** relative to **4** arises apparently from charge-assisted hydrogen bonds involving a tethered ammonium group that not only provides electrostatic attraction for the incoming CN^- anion, but also helps stabilize the developing negative charge in the transition-state leading to the product **3a**.[67−69] In addition to this charge effect, the slower response kinetics of **4** toward CN^- might have its origin in the steric constraints imposed by the bulky Boc substituent on the terminal amine group.

Internal bond rotations facilitate nonradiative decay of dye molecules in the excited-states.[46,47] Binding-induced restriction of such torsional motions results in fluorescence enhancement. Signal transduction mechanisms capitalizing on structural rigidification have previously been implemented with synthetic receptor molecules built on fluorogenic π-systems.[70−74] In a similar manner, the tight hydrogen-bonding network in **3a** should provide additional structural rigidity to the fluorogenic π-backbone and give rise to a larger net turn-on response than the corresponding cyanohydrin adduct of **4** (Figure 7). In support of this notion, the emission quantum yield of the control compound **12**,[75,76] having a π-conjugated backbone identical to that of **3a** but lacking the conformational lock provided by the hydrogen bonds, is only 1.8% in H_2O.[77] This value is significantly lower than that ($\Phi_F = 10\%$) of **3a**.

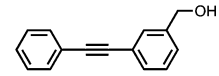

12

Practical Considerations for Cyanide Detection: pH Window, Sensitivity, and Selectivity. Reactivity-based detection of cyanide ion by **3** can be operated in a wide pH range of 6−8, with consistently large fluorescence enhancement (Figure 8a,b).[78] The detection limit at pH = 7.0 was estimated by a

(66) ^{1}H NMR spectra of **5** (4.5 mM) in DMSO-d_6 taken prior to and after treatment of NaCN (5 equiv) are essentially identical, which further confirms the lack of reactivity in the absence of intramolecular hydrogen bonds.

(67) When the Taft equation[68] was used, the pK_a of the ammonium functionality in **3** is estimated to be 8.0, which is close to the value pK_a = 7.96, experimentally determined for the HCl salt of *N*-glycylaniline.[69] The C═O···H−N hydrogen bond in **3** should further enhance the basicity of the terminal amino group. Even a conservative estimation of pK_a = 8.0 suggests that 90% of **3** should exist as the protonated form in water at pH = 7.0.

(68) Perrin, D. D.; Dempsey, B.; Serjeant, E. P. *pK_a Prediction for Organic Acids and Bases*; Chapman and Hall: Cambridge, U.K., 1981.

(69) Peters, F. B.; Johnson, H. W., Jr. *J. Org. Chem.* **1975**, *40*, 1517–1519.

(70) Sandanayake, K. R. A. S.; Nakashima, K.; Shinkai, S. *J. Chem. Soc., Chem. Commun.* **1994**, 1621–1622.

(71) (a) McFarland, S. A.; Finney, N. S. *J. Am. Chem. Soc.* **2001**, *123*, 1260–1261. (b) McFarland, S. A.; Finney, N. S. *J. Am. Chem. Soc.* **2002**, *124*, 1178–1179.

(72) Yamada, K.; Nomura, Y.; Citterio, D.; Iwasawa, N.; Suzuki, K. *J. Am. Chem. Soc.* **2005**, *127*, 6956–6957.

(73) Jiang, X.; Vieweger, M. C.; Bollinger, J. C.; Dragnea, B.; Lee, D. *Org. Lett.* **2007**, *9*, 3579–3582.

(74) Opsitnick, E.; Lee, D. *Chem.—Eur. J.* **2007**, *13*, 7040–7049.

(75) Matsunaga, N.; Kaku, T.; Itoh, F.; Tanaka, T.; Hara, T.; Miki, H.; Iwasaki, M.; Aono, T.; Yamaoka, M.; Kusaka, M.; Tasaka, A. *Bioorg. Med. Chem.* **2004**, *12*, 2251–2273.

(76) ^{1}H NMR (400 MHz, $CDCl_3$, 298 K): δ 7.52−7.55 (m, 3H), 7.46−7.48 (m, 1H), 7.34−7.37 (m, 5H). ^{13}C NMR (100 MHz, $CDCl_3$, 298 K): δ 141.2, 131.8, 130.9, 130.2, 128.7, 128.5, 128.5, 126.9, 123.7, 123.3, 89.7, 89.3, 65.1.

(77) Fluorescence quantum yield of diphenylacetylene is only 0.34% at 298 K. See: Ferrante, C.; Kensy, U.; Dick, B. *J. Phys. Chem.* **1993**, *97*, 13457−13463.

(78) For a wider pH window, a phosphate buffer system was used instead of HEPES. As shown in Figure 8c,d, **3** does not respond to $H_2PO_4^-$ in water.

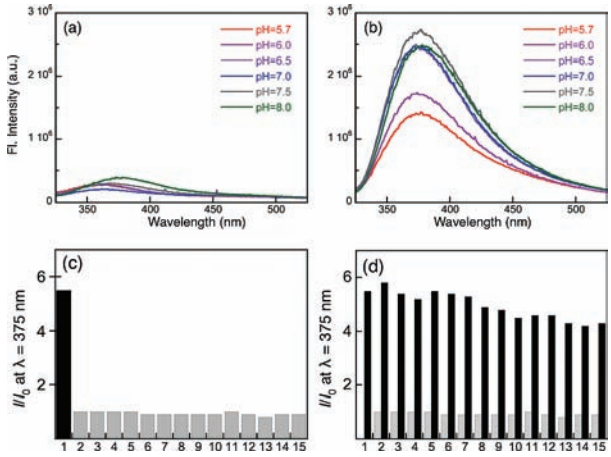

Figure 8. (a) Emission spectra of **3** (5.0 μM) in H_2O at various pH values (5.7−8.0, phosphate, 0.2 M), and (b) fluorescence enhancement after addition of NaCN (1.5 mM). (c) Fluorescence response of **3** (5.0 μM) to various anions in water at pH = 7.0 (HEPES, 10 mM). The signal intensity (I) at λ = 375 nm is normalized with that of the untreated probe (I_0). The bars represent the emission (= I/I_0) of **3** in the presence of 300 equiv of the anion of interest: 1, CN^-; 2, F^-; 3, Cl^-; 4, Br^-; 5, I^-; 6, HSO_4^-; 7, N_3^-; 8, HCO_3^-; 9, PF_6^-; 10, $H_2PO_4^-$; 11, OH^-; 12, ClO_4^-; 13, AcO^-; 14, NO_3^-; 15, SCN^-, all delivered as sodium salts. (c) The selectivity of **3** for cyanide in the presence of other anions. The light gray bars represent the emission of **3** in the presence of 300 equiv of the anion of interest. The black bars indicate the change in the emission that occurs upon subsequent addition of 300 equiv of cyanide to the solution containing **3** and the anion of interest. λ_{exc} = 270 nm; T = 298 K.

plot of ΔI_{375nm} versus cyanide concentration, which shows a nice linear correlation down to the value of 2.5 μM (Figure S10). This value is comparable to the WHO guideline of 0.07 mg/L (= 2.7 μM) cyanide in drinking water.[79] Besides sensitivity, selectivity is another important criteria in cyanide detection. As noted in previous studies, competitive binding[44] or nucleophilic attack[15a,b,d] by fluoride or acetate ion compromised the practical utility of certain cyanide sensory systems. As shown in Figure 8c, among 15 different anions screened, including F^-, Cl^-, Br^-, I^-, HSO_4^-, N_3^-, HCO_3^-, PF_6^-, $H_2PO_4^-$, OH^-, ClO_4^-, AcO^-, NO_3^-, and SCN^-, **3** responds exclusively to cyanide in water at pH = 7.0 (HEPES, 10 mM). This excellent selectivity was further highlighted by competition experiments (Figure 8d), in which a consistent turn-on fluorescence response (>5-fold) was observed upon addition of cyanide to sample solutions of **3** containing equal concentrations of potentially competing anions.

Summary and Outlook

A mechanism-based turn-on fluorescence probe was prepared that responds exclusively to cyanide in water at pH = 6−8. In our structure design, a 2,2′-functionalized diphenylacetylene motif was employed to introduce multiple (and positively charged) N−H groups, which converge at the carbonyl group and activate it for cyanide capture. The functional relevance of such charge-assisted bifurcated hydrogen bonding was established through comparative studies on a set of structural analogues built on the common π-conjugated molecular scaffold.

Unlike existing CN^- probes that have a single O−H/N−H group installed α or β to the carbonyl group (Scheme 1), the use of synthetic β-turn mimic here significantly alleviates the restrictions on the structure and number of hydrogen-bonding donor groups that activate the carbonyl group for the reactivity-based detection of cyanide. In addition, an effective structural "decoupling" of the fluorophore, activator, and receptor component (Scheme 2) should facilitate structure optimization of this proof-of-principle probe through a highly modular synthetic route (Scheme 3). The logical next step is improving the sensitivity and optical properties (i.e., longer wavelength emission and higher quantum yield) of this first-generation molecular prototype, which is the topic of ongoing research in our laboratory.

Experimental Section

General Considerations. All reagents were obtained from commercial suppliers and used as received unless otherwise noted. The solvents MeCN, THF, and dichloromethane were saturated with nitrogen and purified by passage through activated Al_2O_3 columns under nitrogen (Innovative Technology SPS 400). All water used in this study was purified by an E-pure water filtration system (Barnstead Thermolyne Co.). The compounds methyl 4-amino-3-iodobenzoate (**6**),[80] 2-iodobenzaldehyde,[81] 3-(*tert*-butoxycarbonylamino)propanoic acid (Boc-Gly-OH),[82] and (3-ethynylphenyl)methanol (**11**)[83] were prepared according to literature procedures. The synthesis of (3-(2-phenylethynyl)phenyl)methanol (**12**) has previously been reported.[72] All air-sensitive manipulations were carried out under nitrogen atmosphere by standard Schlenk-line techniques.

Physical Measurements. ^1H and ^{13}C NMR spectra were recorded on a 300 MHz Varian Gemini 2000 or a 400 MHz Varian Inova NMR Spectrometer. Chemical shifts were reported versus tetramethylsilane and referenced to the residual solvent peaks. High resolution chemical ionization (CI; using CH_4 as CI reagent) and electrospray ionization (ESI) mass spectra were obtained on a Thermo Electron Corporation MAT 95XP-Trap. High resolution GC-MS (CI, using CH_4 as CI reagent) was obtained on a Thermo Electron Corporation MAT 95XP-Trap. FT-IR spectra were recorded on a Nicolet Avatar 360 FT-IR spectrometer with EZ OMNIC ESP software. UV−vis spectra were recorded on a Varian Cary 5000 UV−vis-NIR spectrophotometer. Fluorescence spectra were recorded on a Photon Technology International QM-4-CW Spectrofluorometer with FeliX32 software.

Fluorescence Quantum Yield Measurements. Quantum yields were determined by standard methods,[84] using *p*-terphenyl (Φ_F = 0.93 in cyclohexane solution)[85,86] as a standard. The sample absorbance was maintained less than 0.1 to minimize internal absorption and corrections were made to account for the differences in solvent refractive indexes.

Reactivity Studies. Stock solutions of **3**−**5** in DMSO (2−7 mM) were diluted with either buffered H_2O (pH = 7.0, 10 mM HEPES) or MeCN to prepare sample solutions (5−50 μM). Anion stock solutions (150 mM) of CN^-, F^-, Cl^-, Br^-, I^-, HSO_4^-, N_3^-, HCO_3^-, PF_6^-, $H_2PO_4^-$, OH^-, ClO_4^-, AcO^-, NO_3^-, and SCN^- were prepared by dissolving the corresponding sodium salt in buffered water (pH = 7.0, 10 mM HEPES). To minimize dilution effects, 3−40 μL aliquots of the anion stock solution, corresponding to 30−400 equiv of the substrate, were delivered using microsyringes into a 3.0 mL sample solution placed in a thermostatted Peltier cuvette holder.

(79) *Guidelines for drinking-water quality*; 3rd ed.; World Health Organization: Geneva, 2004. Also available at http://www.who.int/water_sanitation_health/dwq/guidelines/en/.

(80) Finaru, A.; Berthault, A.; Besson, T.; Guillaumet, G.; Berteina-Raboin, S. *Tetrahedron Lett.* **2002**, *43*, 787–790.
(81) Kurono, N.; Honda, E.; Komatsu, F.; Orito, K.; Tokuda, M. *Tetrahedron* **2004**, *60*, 1791–1801.
(82) Fiakpui, C. Y.; Knaus, E. E. *Can. J. Chem.* **1987**, *65*, 1158–1161.
(83) Zhang, Q.; Takacs, J. M. *Org. Lett.* **2008**, *10*, 545–548.
(84) Williams, A. T. R.; Winfield, S. A.; Miller, J. N. *Analyst* **1983**, *108*, 1067–1071.
(85) Pavlopoulos, T. G.; Hammond, P. R. *J. Am. Chem. Soc.* **1974**, *96*, 6568–6579.
(86) Berlman, I. B. *Handbook of fluorescence spectra of aromatic molecules*; Academic Press: New York, 1971.

Kinetic Measurements. Solution samples (5.0 μM) of **3** and **4** were prepared by diluting the DMSO stock solutions (2−7 mM) with either buffered water (pH = 7.0, 10 mM HEPES) or MeCN. Time-dependent changes in the fluorescence intensity were monitored at 375 nm (λ_{exc} = 270 nm) at 288 K (for measurements in MeCN) or 298 K (for measurements in water) with constant stirring. The ΔI versus t kinetic traces were fitted by nonlinear regression method (OriginPro 8) using eq 1, in which the parameters k' (= $k[CN^-]_0$) and I (= intensity at $t \rightarrow \infty$) were allowed to vary.

Methyl 4-Amino-3-((trimethylsilyl)ethynyl)benzoate (7). An oven-dried round-bottom flask was loaded with **6** (1.14 g, 4.12 mmol), $Pd(PPh_3)_2Cl_2$ (78 mg, 0.11 mmol), and CuI (70 mg, 0.37 mmol). The headspace was purged with nitrogen and a premixed solvent (100 mL, $^iPr_2NH$/THF = 1:2, v/v) was delivered under nitrogen to the reaction vessel. A portion of trimethylsilylacetylene (= TMSA; 1.0 mL, 7.1 mmol) was added, and the mixture was stirred for 2 h at r.t. The crude reaction mixture was diluted with EtOAc (100 mL) and the organic layer was washed with an aq solution of EDTA (1 M, 3 × 5 mL) and satd aq solution of $NaHCO_3$ (3 × 20 mL), dried over anhyd $MgSO_4$, and filtered. Volatile fractions were removed under reduced pressure and the residual material was purified by flash column chromatography on SiO_2 (hexanes/EtOAc = 4:1, v/v) to furnish **6** as a pale yellow solid (0.835 g, 82%). ^{1}H NMR (300 MHz, $CDCl_3$, 298 K): δ 8.01 (d, J = 1.6 Hz, 1H), 7.76−7.80 (dd, J = 8.5, 1.6 Hz, 1H), 6.64−6.66 (d, J = 8.5 Hz, 1H), 4.67 (br s, 2H), 3.84 (s, 3H), 0.26 (s, 9H). ^{13}C NMR (75 MHz, $CDCl_3$, 298 K): δ 166.6, 152.0, 134.7, 131.7, 119.3, 113.3, 107.1, 100.7, 100.6, 51.8, 0.2. FT-IR (thin film on NaCl, cm^{-1}): 3481, 3356, 3209, 2955, 2147, 1704, 1627, 1439, 1340, 1324, 1247, 843, 761. HRMS (CI) calcd for $C_{13}H_{17}NO_2Si$ $[M]^+$, 247.1029; found, 247.1016.

(4-Amino-3-((trimethylsilyl)ethynyl)phenyl)methanol (8). To a stirred solution of **7** (0.493 g, 1.99 mmol) in THF (20 mL) at 0 °C was added portionwise $LiAlH_4$ (0.075 g, 1.98 mmol), and the headspace was sparged with nitrogen. After stirring for 2 h at 0 °C, the reaction was quenched with H_2O (0.3 mL) and an aq solution of NaOH (15%, w/w, 0.1 mL). The organic layer was separated, dried over anhyd $MgSO_4$, and filtered. Volatile fractions were removed under reduced pressure and the residual material was purified by flash column chromatography on SiO_2 (hexanes/EtOAc = 3:1, v/v) to furnish **8** as a pale yellow solid (0.341 g, 78%). ^{1}H NMR (300 MHz, $CDCl_3$, 298 K): δ 7.28−7.29 (d, J = 1.8 Hz, 1H), 7.09−7.13 (dd, J = 8.2, 1.8 Hz, 1H), 6.65−6.67 (d, J = 8.2 Hz, 1H), 4.49 (s, 2H), 4.25 (br s, 2H), 1.70 (br s, 1H), 0.26 (s, 9H). ^{13}C NMR (75 MHz, $CDCl_3$, 298 K): δ 147.9, 131.5, 130.4, 129.5, 114.5, 107.9, 101.7, 100.0, 65.0, 0.3. FT-IR (thin film on NaCl, cm^{-1}): 3352, 2923, 2853, 1687, 1591, 1530, 1422, 1274, 1267, 750, 668. HRMS (CI) calcd for $C_{12}H_{17}NOSi$ $[M]^+$, 219.1079; found, 219.1068.

(4-Amino-3-ethynylphenyl)methanol (9). To a stirred solution of **8** (0.257 g, 1.17 mmol) in THF (5 mL) was added water (0.1 mL) and a THF solution of TBAF (2.0 mL, 1.0 M). The reaction was heated at 50 °C for 2.5 h and quenched by adding satd aq solution (25 mL) of $NaHCO_3$. The organic layer was separated, dried over anhyd $MgSO_4$, and filtered. Volatile fractions were removed under reduced pressure and the residual material was purified by flash column chromatography on SiO_2 (CH_2Cl_2/EtOAc = 10:1, v/v) to furnish **9** as a pale yellow oil (0.173 g, >99%). ^{1}H NMR (300 MHz, $CDCl_3$, 298 K): δ 7.32 (d, J = 1.6 Hz, 1H), 7.14−7.18 (dd, J = 8.2, 1.6 Hz, 1H), 6.68−6.70 (d, J = 8.2 Hz, 1H), 4.52 (s, 2H), 4.27 (br s, 2H), 3.38 (s, 1H), 1.58 (br s, 1H). ^{13}C NMR (75 MHz, $CDCl_3$, 298 K): δ 148.3, 131.9, 130.5, 129.8, 114.6, 106.7, 82.7, 80.5, 65.1. FT-IR (thin film on NaCl, cm^{-1}): 3393, 3313, 2955, 2879, 2548, 1617, 1577, 1423, 1259, 1020, 833, 750, 668. HRMS (CI) calcd for C_9H_9NO $[M]^+$, 147.0684; found, 147.0679.

***tert*-Butyl-2-(2-ethynyl-4-(hydroxymethyl)phenylamino)-2-oxoethylcarbamate (10).** To a stirred CH_2Cl_2 solution (10 mL) of **9** (0.106 g, 0.717 mmol) and EDC (0.151 g, 0.790 mmol) at 40 °C was added slowly Boc-Gly-OH[79] (0.161 g, 0.848 mmol). After stirring for 2 h at 40 °C, the reaction mixture was diluted with EtOAc (100 mL), washed with satd aq solution (3 × 25 mL) of $NaHCO_3$, dried over anhyd $MgSO_4$, and filtered. Volatile fractions were removed under reduced pressure and the residual material was purified by flash column chromatography on SiO_2 (CH_2Cl_2/EtOAc = 3:1, v/v) to isolate **10** as a pale yellow solid (0.835 g, 83%). ^{1}H NMR (300 MHz, $CDCl_3$, 298 K): δ 8.65 (br s, 1H), 8.38−8.41 (d, J = 8.5 Hz, 1H), 7.47−7.48 (d, J = 1.8 Hz, 1H), 7.33−7.36 (dd, J = 8.5, 1.8 Hz, 1H), 5.19 (br s, 1H), 4.63 (s, 2H), 3.97−3.98 (d, 2H), 3.49 (s, 1H), 1.82 (br s, 1H), 1.47 (s, 9H). ^{13}C NMR (75 MHz, $CDCl_3$, 298 K): δ 168.1, 156.1, 138.2, 136.6, 130.6, 128.9, 119.3, 111.2, 84.6, 80.7, 78.9, 64.2, 45.4, 28.5. FT-IR (thin film on NaCl, cm^{-1}): 3349, 2978, 1684, 1590, 1521, 1418, 1368, 1251, 1164, 1050, 831, 660. HRMS (CI) calcd for $C_{16}H_{20}N_2O_4$ $[M]^+$, 304.1423; found, 304.1417.

***tert*-Butyl-2-(2-((2-formylphenyl)ethynyl)-4-(hydroxy-methyl)-phenylamino)-2-oxoethylcarbamate (4).** This compound was prepared using **10** (0.454 g, 1.49 mmol), 2-iodobenzaldehyde (0.438 g, 1.89 mmol), $Pd(PPh_3)_2Cl_2$ (54 mg, 0.077 mmol), and CuI (28 mg, 0.15 mmol) in a manner similar to that described for **7**. After stirring for 6.5 h at r.t., the reaction mixture was diluted with EtOAc (100 mL), washed with aq solution (1 M) of EDTA (3 × 5 mL) and satd aq solution (3 × 5 mL) of $NaHCO_3$, dried over anhyd $MgSO_4$, and filtered. Volatile fractions were removed under reduced pressure and the residual material was purified by flash column chromatography on SiO_2 (CH_2Cl_2/EtOAc = 3:1, v/v) to furnish **4** as a yellow solid (0.560 g, 92%). ^{1}H NMR (300 MHz, $CDCl_3$, 298 K): δ 10.10 (s, 1H), 9.38 (br s, 1H), 8.40−8.43 (d, J = 8.5 Hz, 1H), 7.76−7.79 (d, J = 7.3 Hz, 1H), 7.49−7.64 (m, 4H), 7.26−7.30 (d, J = 8.7 Hz, 1H), 5.50 (br s, 1H), 4.61 (s, 2H), 4.24−4.25 (d, 2H), 2.61 (br s, 1H), 1.40 (s, 9H). ^{13}C NMR (75 MHz, $CDCl_3$, 298 K): δ 191.8, 168.7, 156.2, 139.3, 136.4, 135.3, 134.0, 133.9, 130.7, 129.2, 128.7, 122.5, 119.8, 116.3, 111.7, 94.0, 90.9, 80.0, 64.3, 45.0, 28.4. FT-IR (thin film on NaCl, cm^{-1}): 3319, 2977, 2929, 1643, 1589, 1522, 1291, 1165, 1052, 762. HRMS (CI) calcd for $C_{23}H_{24}N_2O_5$ $[M]^+$, 408.1685; found, 408.1670.

2-(2-((2-Formylphenyl)ethynyl)-4-(hydroxymethyl)-phenylamino)-2-oxoethanaminium chloride (3). A stream of HCl gas, generated by using a concd H_2SO_4 (15 mL) trap, was bubbled through a stirred CH_2Cl_2 solution (50 mL) of **4** (0.0436 g, 0.121 mmol) at 0 °C. After stirring for 5 min, the crude product was isolated by filtration and washed with CH_2Cl_2 (200 mL) to isolate **3** as a pale yellow solid (0.0419 g, 99%). ^{1}H NMR (300 MHz, DMSO-d_6, 298 K): δ 10.44 (s, 1H), 10.16 (s, 1H), 8.40 (br s, 3H), 7.96−7.98 (d, J = 7.7 Hz, 1H), 7.85−7.87 (m, 2H), 7.76−7.79 (m, 1H), 7.63−7.67 (m, 2H), 7.41−7.43 (d, J = 8.5 Hz, 1H), 4.51 (s, 2H), 3.96 (s, 2H). ^{13}C NMR (75 MHz, DMSO-d_6, 298 K): δ 192.1, 165.4, 139.6, 137.0, 135.3, 134.3, 133.7, 130.4, 129.6, 129.4, 128.3, 124.1, 122.9, 114.3, 91.7, 91.4, 61.9, 40.9. FT-IR (thin film on NaCl, cm^{-1}): 3275, 2975, 2861, 2682, 2601, 2206, 1967, 1684, 1460, 1365, 1290, 1198, 1065, 911, 766, 658. HRMS (ESI) calcd for $C_{18}H_{17}N_2O_3$ $[M - Cl]^+$, 309.1239; found, 309.1249.

2-((3-(Hydroxymethyl)phenyl)ethynyl)benzaldehyde (5). This compound was prepared using **11** (0.338 g, 2.56 mmol), 2-iodobenzaldehyde (0.596 g, 2.57 mmol), $Pd(PPh_3)_2Cl_2$ (83 mg, 0.12 mmol), and CuI (41 mg, 0.22 mmol) in a manner similar to that described for **7**. After stirring for 1.5 h at r.t., the reaction mixture was diluted with EtOAc (100 mL), washed with aq solution (1 M) of EDTA (3 × 25 mL) and satd aq solution (3 × 25 mL) of $NaHCO_3$, dried over anhyd $MgSO_4$, and filtered. Volatile fractions were removed under reduced pressure and the residual material was purified by flash column chromatography on SiO_2 (CH_2Cl_2/EtOAc = 10:1, v/v) to furnish **5** as a yellow solid (0.470 g, 78%). ^{1}H NMR (400 MHz, $CDCl_3$, 298 K): δ 10.58 (s, 1H), 7.89−7.91 (d, J = 7.6 Hz, 1H), 7.53−7.60 (m, 3H), 7.40−7.45 (m, 2H), 7.31−7.35 (m, 2H), 4.67 (s, 2H), 2.74 (br s, 1H). ^{13}C NMR (75 MHz, $CDCl_3$, 298 K): δ 191.9, 141.5, 135.8, 133.9, 133.3, 130.8, 130.0, 128.7, 128.7, 127.6, 127.4, 126.8, 122.5, 96.3, 85.0, 64.6.

FT-IR (thin film on NaCl, cm^{-1}): 3377, 2849, 1693, 1593, 1489, 1268, 1192, 1033, 761, 690, 638. HRMS (CI) calcd for $C_{16}H_{12}O_2$ $[M]^+$, 236.0837; found, 236.0842.

Acknowledgment. This work was supported by the U.S. Army Research Office (W911NF-07-1-0533) and the National Science Foundation (CAREER CHE 0547251). D.L. is an Alfred P. Sloan Research Fellow. We thank Dr. Ho Yong Lee for helpful discussions and Soumya Ghosh of the Baik group at Indiana University for assistance in DFT studies.

Supporting Information Available: Additional spectroscopic and kinetic data. This material is available free of charge via the Internet at http://pubs.acs.org.

JA907056M